Inorganic Chemistry
Article
pubs.acs.org/IC

Potassium, Cesium, and Ammonium Peroxogermanates with Inorganic Hexanuclear Peroxo Bridged Germanium Anion Isolated from Aqueous Solution

Alexander G. Medvedev,[†,‡] Alexey A. Mikhaylov,[†,‡] Andrei V. Churakov,[†] Mikhail V. Vener,[†] Tatiana A. Tripol'skaya,[†] Shmuel Cohen,[‡] Ovadia Lev,[*,‡] and Petr V. Prikhodchenko[*,†]

[†]Kurnakov Institute of General and Inorganic Chemistry, Russian Academy of Sciences, Leninskii prosp. 31, Moscow 119991, Russia
[‡]The Casali Center of Applied Chemistry, The Institute of Chemistry, The Hebrew University of Jerusalem, Jerusalem 91904, Israel

Ⓢ *Supporting Information*

ABSTRACT: Potassium ($K_6[Ge_6(\mu\text{-}OO)_6(\mu\text{-}O)_6(OH)_6]\cdot 14H_2O$, **1**), cesium ammonium ($(Cs_{4.2}(NH_4)_{1.8}[Ge_6(\mu\text{-}OO)_6(\mu\text{-}O)_6(OH)_6]\cdot 8H_2O$, **2**), and potassium ammonium ($(K_{2.4}(NH_4)_{3.6}[Ge_6(\mu\text{-}OO)_6(\mu\text{-}O)_6(OH)_6]\cdot 6H_2O$, **3**) peroxogermanates were isolated from 3% hydrogen peroxide aqueous solutions of the corresponding hydroxogermanates and characterized by single crystal and powder X-ray diffraction studies and by Raman spectroscopy and thermal analysis. The crystal structure of all three compounds consists of cations of potassium and/or ammonium and cesium, water molecules, and centrosymmetric hexanuclear peroxogermanate anion $[Ge_6(\mu\text{-}OO)_6(\mu\text{-}O)_6(OH)_6]^{6-}$ with six μ-oxo- and six μ-peroxo groups. Peroxogermanates demonstrate relatively high thermal stability: the peroxide remains in the structure even after water release after heating to 100−120 °C. DFT calculations of the peroxogermanate $[Ge_6(\mu\text{-}OO)_6(\mu\text{-}O)_6(OH)_6]^{6-}$ anion confirm its higher thermodynamic stability compared to the hydroperoxo- and oxogermanate analogues.

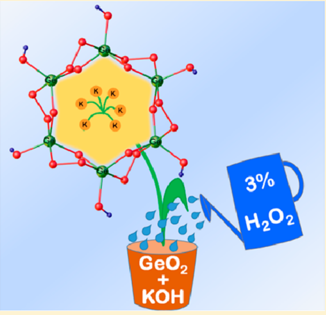

INTRODUCTION

Gels, sol gel materials, and soft matter in general have increasing contemporary importance. Hydrogen peroxide addition is known to induce polycondensation and gelation of transition and nontransition element oxides in aqueous solutions.[1−3] This process can be used for sol and film formation, which can serve as end products or as solid oxide, sulfide, and Ormocer precursors.[1,4−8]

Three mechanisms may be responsible for the hydrogen peroxide enhanced polymerization: (i) Hydrogen peroxide is acidic and induces polycondensation by oxo- or hydroxo-bridging. (ii) Hydrogen peroxide is a superior hydrogen donor compared to water,[9] and its rotation around the O−O axis provides flexibility and optimal orientation both of which contribute to stronger hydrogen bonding.[10−12] (iii) Peroxo bridging can participate in or form by itself, without contributing oxo bridging, the skeleton of the gel, or soft matter.

For inorganic oxides, hydrogen bonding alone would not be sufficient to hold together a solid network, which leaves two dominant polymerization mechanisms, (i) and (iii). The mere possibility of peroxo bridging of multinuclear elements in aqueous solution is still questionable. When the peroxide rich product is a soft matter, its structure elucidation is challenging. Structure elucidation of soft matter comprised of noncrystalline peroxides is challenging even with state of the art spectroscopy and diffraction methods. For example, “persilicate”, a useful commodity and a product of peroxide induced polymerization of sodium metasilicate, is amply discussed in the literature[2,13−15] with stipulations regarding the possibility of peroxo coordination, and the same holds for peroxostannate[3] and peroxoantimonate[16] gels. In contradistinction, crystal structure studies of polynuclear peroxocompounds can shed light on the skeletal polymer and its building blocks when crystal structure can be shown to reflect the solution chemistry.

Peroxo bridged dinuclear peroxocomplexes were reported for many transition metals, including manganese,[17−19] iron,[20−24] cobalt,[25−32] nickel,[33] copper,[34−36] rhodium,[37] palladium,[38,39] iridium,[40] platinum,[41] tungsten,[42] and recently even gold.[43] However, we could find only two reports of multinuclear μ-O−O transition metal peroxocomplexes. Bassil et al.[44] reported $[Zr_6(O_2)_6(OH)_6(\text{-}SiW_{10}O_{36})_3]^{18-}$, a six nuclear peroxo bridged complex, and its Hf analogue. Chernyshev et al.[45] reported a peroxo bridged cyclic trimer $Zr_3F_{12}(O_2)_3$. All three polynuclear complexes were isolated from aqueous solutions. All three have side-on $\mu\text{-}\eta^2{:}\eta^2\text{-}O_2^{\,2-}$ peroxide coordination, which is possible for d-elements but improbable for p-block elements. Crystallographically described p-block element peroxocomplexes have only end-on peroxo bridges and are mainly dimeric.

Dinuclear peroxo metaloorganic compounds of silicon,[46] gallium,[47−49] tin,[50−52] antimony,[53−55] tellurium,[56] bismuth,[57] and boron[58] have been reported. The peroxoborates are the only strictly inorganic dinuclear μ-O−O p-block element compounds, and they are the only p-block element peroxo bridged compounds that were isolated from aqueous solution.

Received: June 9, 2015
Published: August 4, 2015

DOI: 10.1021/acs.inorgchem.5b01293
Inorg. Chem. 2015, 54, 8058−8065

Dinuclear peroxo bridged germanium complexes received considerable attention,[59−63] though they were all isolated from nonaqueous solutions. Based on the Cambridge Structural Database[64] and Inorganic Crystal Structure Database,[65] there is only a single polynuclear peroxo bridged nontransition element compound, trinuclear cyclic tris(dimethylsilyl peroxide),[66] which was obtained from anhydrous ethanol solution by reaction of dichlorodimethylsilane with 99% hydrogen peroxide and ammonia.

We report here on germanium inorganic crystalline peroxocompounds containing a polynuclear end-on peroxo bridged anion, $[Ge_6(\mu\text{-OO})_6(\mu\text{-O})_6(OH)_6]^{6-}$, that is isolated from basic aqueous peroxide solution as potassium ($K_6[Ge_6(\mu\text{-OO})_6(\mu\text{-O})_6(OH)_6]\cdot 14H_2O$, **1**), cesium ammonium ($(Cs_{4.2}(NH_4)_{1.8}[Ge_6(\mu\text{-OO})_6(\mu\text{-O})_6(OH)_6]\cdot 8H_2O$, **2**), and potassium ammonium ($K_{2.4}(NH_4)_{3.6}[Ge_6(\mu\text{-OO})_6(\mu\text{-O})_6(OH)_6]\cdot 6H_2O$, **3**) crystalline salts.

EXPERIMENTAL SECTION

Materials. Germanium(IV) chloride, ammonium hydroxide, potassium hydroxide, cesium hydroxide monohydrate, and 50% aqueous hydrogen peroxide were purchased from Aldrich Sigma.

Synthesis. *Preparation of Hydroxogermanate Solution.* Germanium hydroxide was obtained by careful addition of NH_4OH to aqueous solution of 0.75 g (3.5 mmol) of germanium chloride $GeCl_4$ with stirring and pH control. After the pH reached 7, the precipitate was isolated by centrifugation, washed 5 times with water, and dissolved in 3.5 mL of 2 M KOH at 70 °C. The resulting mixture was heated for about 2 h. After complete dissolution of the precipitate, the solution was filtered. The germanium concentration in the resulted potassium hydroxogermanate solution was calculated as 0.7 M from the initial amount of $GeCl_4$ without taking into account the loss of germanium hydroxide during the washing and due to its partial solubility in water.

*Synthesis of $K_6[Ge_6(\mu\text{-OO})_6(\mu\text{-O})_6(OH)_6]\cdot 14H_2O$ (**1**).* One hundred twenty microliters of 50% aqueous H_2O_2 (purchased from Sigma-Aldrich) was added to 1.88 mL of 0.7 M aqueous potassium hydroxogermanate to achieve 3% hydrogen peroxide in the resulting solution. Then the solution was kept in a closed beaker at 4 °C. Colorless crystals were formed after 1 day. They were filtered and washed 3 times with diethyl ether and dried in air for 30 min. Yield 24% (based on Ge). Anal. Calcd for $H_{34}O_{38}K_6Ge_6$ (1): OO (peroxide), 14.63; K, 17.87; Ge, 33.20. Found: OO (peroxide), 14.50; K, 17.2; Ge, 32.8.

*Synthesis of $Cs_{4.2}(NH_4)_{1.8}[Ge_6(\mu\text{-OO})_6(\mu\text{-O})_6(OH)_6]\cdot 8H_2O$ (**2**).* Cesium hydroxogermanate solution (1.5 M) was prepared from $GeCl_4$ by the same method as described above for potassium hydroxogermanate solution. One hundred twenty microliters of 50% H_2O_2 and 1.3 mL of NH_4OH were slowly added to 0.5 mL of 1.5 M cesium hydroxogermanate with stirring. The resulting solution was kept in a closed beaker at 4 °C. Colorless crystals were formed after 1 day. They were filtered and washed 3 times with diethyl ether and dried in air for 30 min. Yield 18% (based on Ge). Anal. Calcd for $Cs_{4.2}Ge_6H_{29.2}N_{1.8}O_{32}$ (**3**): N, 1.62; OO (peroxide), 12.30; Ge, 27.93; Cs, 35.77. Found: N, 1.70; OO (peroxide), 12.30; Ge, 27.1, Cs, 34.9.

*Synthesis of $K_{2.4}(NH_4)_{3.6}[Ge_6(\mu\text{-OO})_6(\mu\text{-O})_6(OH)_6]\cdot 6H_2O$ (**3**).* Two hundred fifty microliters of water, 140 μL of 50% H_2O_2, and 1.2 of NH_4OH were added one by one to 0.75 mL of 0.7 M potassium hydroxogermanate solution with stirring. The resulting solution was kept in a closed beaker at 4 °C. Colorless crystals were formed after 1 day. They were filtered and washed 3 times with diethyl ether and dried in air for 30 min. Yield 21% (based on Ge). Anal. Calcd for $H_{32.4}N_{3.6}O_{30}K_{2.4}Ge_6$ (**2**): N, 4.61; OO (peroxide), 17.57; K, 8.59; Ge, 39.89. Found: N, 4.30; OO (peroxide), 17.10; K, 8.30; Ge, 39.1. Based on XRD studies the same phase was isolated also from 20% H_2O_2.

Interaction of Germanium Chloride with 50% Aqueous Hydrogen Peroxide. $GeCl_4$ (99.9%) (0.5 mL) was introduced into 2 mL of 50% hydrogen peroxide solution under stirring, and gelation was observed. Precipitation was accomplished by addition of 15 mL of ethanol:ether mixture (1:3). The precipitate was washed several times with ether and dried in vacuum desiccator. Peroxide content was not detected in the resulting material (according to permanganometric titration).

Preparation of 98.3 wt % Hydrogen Peroxide. The hydrogen peroxide was prepared from serine perhydrate crystals according to our previously reported protocol.[67]

CAUTION: Concentrated hydrogen peroxide is explosive.

Single Crystal X-ray Analysis. Experimental intensities for **1** and **2** were collected on a Bruker SMART APEX II diffractometer using graphite monochromatized Mo−K*α* radiation (*λ* = 0.710 73 Å). Absorption corrections based on measurements of equivalent reflections were applied. The structures were solved by direct methods and refined by full matrix least-squares on F^2 with anisotropic thermal parameters for all non-hydrogen atoms (*SHELXTL*). In **1**, three water molecules O5/O6, O7/O8, and O9/O10 are disordered over two closely adjacent positions with occupancy ratios 0.88/0.12, 0.50/0.50, and 0.92/0.08, respectively. In **2**, Cs(3) and ammonium cations share the same site with occupancy ratio 0.101(1)/0.899(1). In both structures, all hydrogen atoms were found from difference Fourier synthesis and refined isotropically. In **1**, most of the water molecules were refined with restrained O−H and H···H distances. As for **2**, the ammonium cation was refined with slightly restrained H···H separations (SADI). Details of X-ray studies are given in Table S2. Crystallographic data (excluding structure factors) for the structures **1** and **2** have been deposited with the Cambridge Crystallographic Data Centre as supplementary publication no. CCDC-1054007 and 1054008, respectively. Copies of the data can be obtained free of charge on application to CCDC, 12 Union Road, CambridgeCB2 1EZ, UK [fax: + 44-1223-336-033; e-mail: deposit@ccdc.cam.ac.uk].

X-ray powder diffraction measurements were performed on a D8 Advance diffractometer (Bruker AXS, Karlsruhe, Germany) with a goniometer radius of 217.5 mm, Göbel Mirror parallel-beam optics, 2° Sollers slits, and a 0.2 mm receiving slit. The powder samples were filled into low background quartz sample holders. The specimen weight was 0.5 g. XRD patterns in the range 2°−75° 2*θ* were recorded at room temperature using CuK*α* radiation (*λ* = 1.5418 Å) under the following measurement conditions: Tube voltage of 40 kV, tube current of 40 mA, step scan mode with a step size 0.02° 2*θ*, and counting time of 1s/step. XRD patterns were processed by DiffracPlus software.

Raman Spectroscopy. The measurements were performed at room temperature with a Renishaw inVia Raman microscope. The incident light was 514 nm with a power of 5.0 mW. Regular spectra were acquired with a 20× objective, and the line scan measurements were performed with a 5× objective. The spatial resolution for line scan was 5 μm.

Differential scanning calorimetry (DSC) was performed on differential scanning calorimeter, DSC 822 Mettler, Toledo, and **thermogravimetric analysis** (TGA) was conducted on Thermobalance, TG50 Mettler, Toledo. All experiments were carried out in the range 40−400 °C under nitrogen flow at a heating rate of 5°/min.

^{17}O NMR Spectrometry. ^{17}O NMR spectra were collected on a Bruker Avance-500 (11.7483T) spectrometer at resonance frequency of 67.8 MHz. The measurements were performed using a single pulse sequence with rf pulse duration of 8 μs and recycling time of 0.031 s. Experiments were carried out at 5 °C. The ^{17}O chemical shifts were measured relative to water.

Peroxide, Potassium, Cesium, Germanium and Nitrogen Determination. Peroxide content was estimated by permanganometry. Potassium and cesium content was analyzed by inductively coupled plasma atomic emission spectroscopy on a Thermo Jarrell Ash ICAP-61E instrument according to the EPA method 6010. Germanium content was calculated based on the cation (potassium or cesium)/germanium ratio determined by EDX analysis. Nitrogen content was determined using the PerkinElmer 2400 series II Analyzer.

Computational. Gaussian09 was used in all computations.[68] Geometry of the $[Ge_6(\mu\text{-O})_{12}(OH)_6]^{6-}$, $[Ge_6(\mu\text{-O})_{12}(OOH)_6]^{6-}$, $[Ge_6(\mu\text{-OO})_6(\mu\text{-O})_6(OH)_6]^{6-}$, and $[Ge_6(\mu\text{-OO})_{12}(OH)_6]^{6-}$ anions as well as H_2O and H_2O_2 were optimized at the B3LYP/6-311G++(d,p) level using LANL2DZ basis set with effective core potential for Ge atoms. The normal-mode analysis did not give imaginary frequencies for the considered species. The sum of electronic and thermal free energies[68] was used in evaluation of the relative Gibbs energy $\Delta_rG^0_{298\ K}$ of reactions 1–3.

■ RESULTS AND DISCUSSION

The structure of **1** comprises hexanuclear peroxide-containing anion $[Ge_6(\mu\text{-}OO)_6(\mu\text{-}O)_6(OH)_6]^{6-}$, potassium cations, and water molecules. In centrosymmetric anion, all six germanium atoms possess trigonal bipyramid coordination environment (Figure 1). The apical vertexes are occupied by peroxo ligands, while oxo and hydroxo groups lie on equatorial positions. The angles between the apical substituents are greater than 175.45(5)° (Table S1).

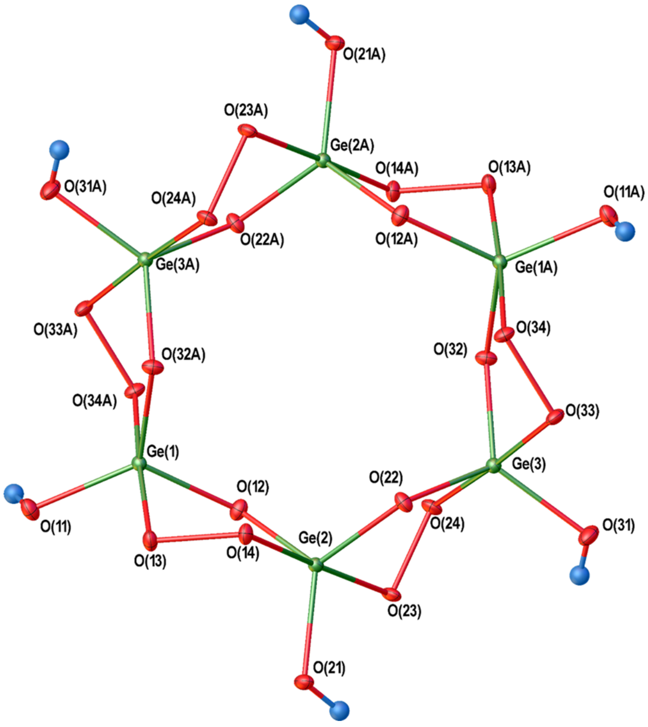

Figure 1. Hexanuclear peroxide-containing anion $[Ge_6(\mu\text{-}OO)_6(\mu\text{-}O)_6(OH)_6]^{6-}$ in the structure **1**. Displacement ellipsoids are drawn at the 50% probability level.

At the same time the equatorial angles are close to 120° (116.83(5)–123.33(5)°), and the angles between apical and equatorial ligands vary within 84.80(5)–95.13(5)°. Displacements of Ge atoms from the least-squares planes of the three equatorial oxygen atoms are less than 0.008 Å (Table S1).

According to CSD data (ver. 5.36, Feb 2015), Ge–OH and Ge–μO distances adopt ordinary values.[64] In contrast, Ge–OO bond lengths (1.884(1)–1.916(1) Å) are noticeably longer than those found in all known complexes in which two germanium atoms are bridged by peroxide (1.76(1)–1.857(5) Å).[59−63] O–O distances (1.490(2)–1.491(1) Å) lie within the range found previously for bridging Ge–O–O–Ge fragments (1.42(1)–1.528(7) Å).[60,63] On the other hand, these values are of about 0.03 Å greater than those previously observed in the accurately determined structures of hydrogen peroxide molecule in crystalline H_2O_2 (1.461(3) Å),[69] urea perhydrate (1.4573(8) Å),[70] and serine perhydrate (1.461(2) Å).[11] All peroxo groups exhibit gauche conformation with Ge–O–O–Ge torsion angles close to 60°.

The neighboring Ge atoms are linked by one μ-oxo and one μ-peroxo ligands forming five-membered metallocycles. All these cycles adopt envelope conformation with both germanium atoms, μ-oxo atom, and one μ-peroxo atom lying in the base plane, while the second peroxo atom occupies the flap site of the envelope. Of interest, all terminal OH groups are directed outward the anion center. Evidently this arrangement facilitates formation of intermolecular hydrogen bonds.

The unit cell of **1** contains three crystallographycally unique potassium atoms. All of them possess irregular coordination polyhedra with coordination number CN equal to 10. Their coordination environment are partially formed by three (for K1) or four (for K2 and K3) oxygen atoms originated from both μ-oxo and μ-peroxo groups of the anions. All other coordination sites are engaged by water molecules. The K–O distances vary within the range 2.6959(14)–3.4254(12) Å. It should be noted that the terminal hydroxo groups HO-Ge do not interact with potassium cations.

The unique part of the unit cell contains seven water molecules. Three of them are disordered over two closely adjacent positions. Six water molecules are coordinated by K cations, while one of them (O9/O10) occupies an outer-sphere position. All water hydrogen atoms are involved in hydrogen bonding.

All six terminal hydroxo ligands of $[Ge_6(\mu\text{-}OO)_6(\mu\text{-}O)_6(OH)_6]^{6-}$ participate in moderate hydrogen bonding with four adjacent anions. The latter results in forming negatively charged layers perpendicular to the *ac*-diagonal (Figure 2A). The space among these layers is filled by potassium cations and water molecules (Figure 3).

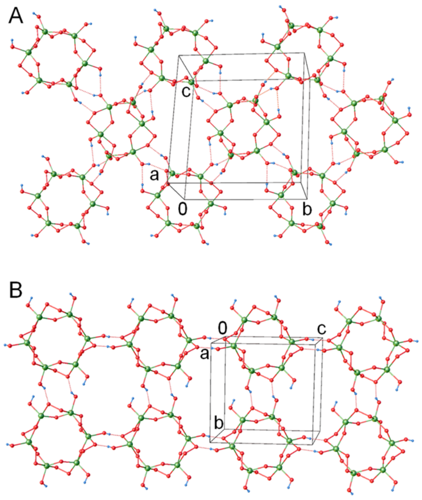

Figure 2. Hydrogen-bonded anion layers in the structure **1** and **2** (A and B, respectively).

The structure **2** consisits of the forementioned $[Ge_6(\mu\text{-}OO)_6(\mu\text{-}O)_6(OH)_6]^{6-}$ anion, Cs and ammonium cations, and water molecules. The geometry of the anions in the crystal structures of **1** and **2** is very similar (Table S1). O–O distances of peroxide ligands are 1.485(2), 1.488(2), and 1.492(2) Å, respectively. Two of three cesium positions (Cs1 and Cs2) are occupied completely by metal, while the third (Cs3) is shared with ammonium cation in the molar ratio of cesium and ammonium 0.10/0.90. The same partial substitution Cs^+/NH_4^+

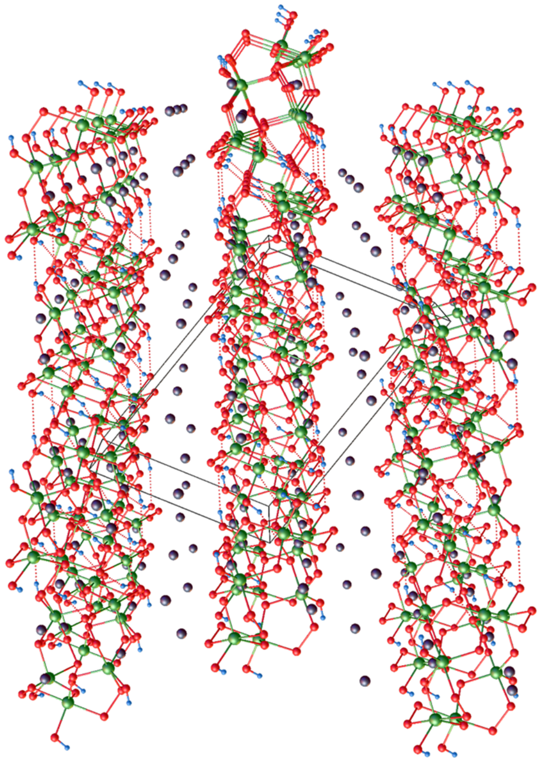

Figure 3. Arrangement of K cations (gray spheres) between anion chains (view along *b*-axis) in the structure of **1**. Water molecules are not shown for clarity.

is well-known for mixed inorganic salts.[71,72] The coordination numbers of all Cs atoms are 10, and they exhibit irregular coordination environment with Cs−O distances varying from 2.824(2) to 3.728(2) Å. All four hydrogen atoms of NH_4^+ cation are involved in hydrogen bonding with anionic peroxo oxygen atoms only. The N···O separations lie within 2.824(2)−2.958(2) Å. In contrast to **1**, all water molecules in **2** are coordinated by cesium cations and form two donor hydrogen bonds with neighboring anion or water oxygen atoms.

In **2**, four of the six terminal hydroxo groups of each anion participate in hydrogen bonding with peroxo ligands of four adjacent $[Ge_6(\mu\text{-}OO)_6(\mu\text{-}O)_6(OH)_6]^{6-}$ anions forming negatively charged layers perpendicular to the *a*-axis (Figure 2B). As in the structure **1**, the space between these layers is filled by cations and water molecules.

We also performed preliminary single crystal X-ray study of compound **3**—$K_{2.4}(NH_4)_{3.6}[Ge_6(\mu\text{-}OO)_6(\mu\text{-}O)_6(OH)_6]\cdot 6H_2O$. It crystallizes in triclinic space group *P*-1 (a = 7.8761(1), b = 10.2772(2), c = 10.3111(2) Å, α = 101.720(2), β = 104.023(2), γ = 108.366(2), Z = 1). It was unambiguously established that **3** contains absolutely the same hexanuclear peroxide-containing anions $[Ge_6(\mu\text{-}OO)_6(\mu\text{-}O)_6(OH)_6]^{6-}$. These anions are combined by hydrogen bonds in layers similar to those found in **2**. However, the high level of disorder of potassium/ammonium cations and water molecules over six crystallographic sites were determined. The molar ratio between potassium and ammonium cations was determined based on results of the elemental analysis and can be specified after the structure refinement. Details of this structure will be published elsewhere.

X-ray powder diffractograms of **1**−**3** are presented in Figure S1. According to XRD studies of **1**−**3**, all powders are crystalline and do not contain a significant amount of amorphous phase. Most reflections in the diffraction pattern of **1** (Figure S1A) are attributed to the structure that was determined by single crystal X-ray analysis, and only a few additional peaks (d = 8.089, 6.822, and 3.117 Å) indicate some unidentified crystalline impurity. We did not find any known hydroxogermanate, chloride, carbonate, or hydroxide phase which could correspond to these reflections. Probably these reflections are attributed to an unreported potassium hydroxogermanate byproduct in sample **1**. X-ray powder diffractograms of **2** and **3** (Figure S1, B and C, respectively) fit well to the X-ray diffraction patterns calculated from X-ray data of corresponding single crystals. Thus, results of the XRD studies confirm that compounds **1**−**3** are the dominant products isolated from 3% hydrogen peroxide aqueous solutions of the corresponding hydroxogermanates.

Raman spectra of **1**−**3** are depicted in Figure S2, and all have a similar profile. Lines with maxima at 855 cm^{-1} and at lower wavenumbers are attributed to vibrations of GeO_5 polyhedra[73−75] and the broad line with a maximum at 3380 cm^{-1} assigned to O−H vibrations. All spectra reveal a quite intensive peak with a maximum at 872, 874, and 874 cm^{-1}, respectively for **1**−**3**, which corresponds to O−O stretching of peroxo groups in the peroxogermanate anion $[Ge_6(\mu\text{-}OO)_6(\mu\text{-}O)_6(OH)_6]^{6-}$. This peak maximum is shifted to the lower wavenumber values compared to solvated and free hydrogen peroxide (880 cm^{-1})[76] similar to those in Raman spectra of peroxoantimonate[16] and crystalline hydroperoxostannates.[3,77,78] In the case of peroxogermanate anion this bathochromic shift can be caused by a noticeable increase (of about 0.02−0.03 Å) in peroxide bond length as compared to the free H_2O_2 molecule. In addition, the reduction of the wavenumber corresponding to O−O vibrations can also occur due to the relatively heavy atom bonded to the oxygen atom of peroxo group. Therefore, the bathochromic shift of the Raman line corresponding to O−O stretching can be considered as a general spectral characteristic of peroxide or hydroperoxide ligands of main group element peroxocomplexes.

The temperature dependent stability of the peroxogermanates **1**−**3** was characterized by differential scanning calorimetry (DSC) and thermogravimetry (TG) and by direct analysis of the temperature dependent residual peroxide content (by permanganate titration). Results of thermal stability studies of peroxogermanate are depicted in Figure 4A. We also performed Raman studies of the heated samples of **1** and **2**. The Raman spectra in the range corresponding to O−O stretching of **1** heated at different temperatures are depicted in Figures 4B and S2C, D. All four dynamic tests were carried out at a constant temperature scan rate, 5°/min. The DSC curve (Figure 4A, inset) showed a pronounced endothermic peak, starting at 36, 43, and 54 °C and peaking at 40, 51, and 75 °C, for **1**−**3**, respectively, which corresponds to solvated water release. A second, exothermic peak was observed starting at 110, 103, and 129 °C and peaking at 121, 111, and 139 °C, respectively for **1**−**3**. This peak is attributed to peroxide decomposition and oxygen evolution. The TGA data show a first pronounced weight loss starting at 39, 47, and 60 °C, respectively, with good correspondence of the integral weight loss to the solvated water amount in **1**−**3**. The second integral weight loss, starting at 103, 103, and 121 °C, respectively for **1**−**3**, correlates well to the oxygen, water (and ammonia in case of **2** and **3**) evolution that occurred after peroxogermanate decomposition. The Raman line of O−O vibrations remains even after heating of

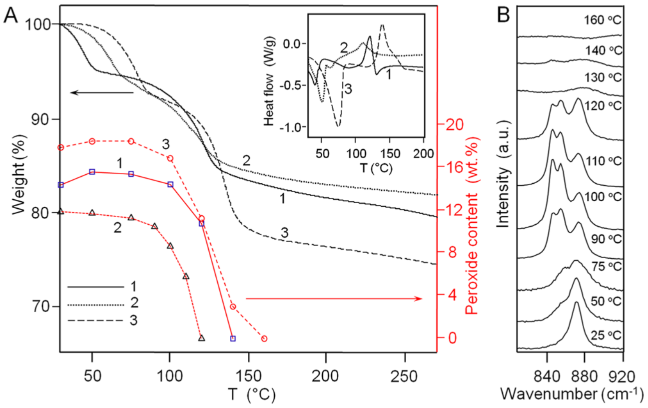

Figure 4. Thermal analyses of peroxogermanates **1**−**3**. On the left (A): Thermogravimetry (black curves) and loss of the peroxide content as a function of temperature (red curves) of **1**−**3**. Insert: Dynamic scanning calorimetry of **1**−**3**. On the right (B): Raman spectrum in the range of O−O stretching of **1** before and after heating at different temperatures.

1 and **2** up to 120 °C, and two additional peaks at 847 and 855 cm^{-1} appear in the Raman spectrum of **1** after heating to 50 °C (Figure 4B). Similar peaks at 853−865 cm^{-1} exist in spectra of **2** and **3** at room temperature (Figure S2B, E), and they can be attributed to stretching modes of Ge−O bond[73−75] which can be inactive in **1** before heating due to the hydrogen bonding to solvated water molecules. Thus, based on the thermal studies we can conclude that peroxogermanate anion is relatively stable. It does not decompose during water release and remains in the structure even when heating up to 120−130 °C. The presence of ammonium in the structures of **2** and **3** increases their thermal stability.

^{17}O NMR studies of a germanate solution before and after addition of 3% hydrogen peroxide are depicted in Figure S3a. Besides the intensive signal of water, the ^{17}O NMR spectrum of initial aqueous hydroxogermanate solution contains a broad peak at 67.1 ppm, which can be attributed to oxo- and hydroxo ligands coordinated to germanium in hydroxogermanate anions. The intensity of this signal (determined by normalization versus water signal) decreased 2 times after addition of 8% hydrogen peroxide solution to the initial germanate solution, and the peak of peroxide appeared at 219.7 ppm (Figure S3b). Most probably, the shift of peroxide compared to ^{17}O NMR spectrum of pure hydrogen peroxide (180 ppm) is induced by deprotonation of H_2O_2 molecules at high pH and does not prove peroxide coordination to germanium.

The same shift of peroxide ^{17}O NMR signal to the weak field occurs in the spectrum of 1 M sodium alkali solution in 4% aqueous hydrogen peroxide (Figure S3c). However, the significant intensity decrease of the signal assigned to the oxo- or hydroxo ligands in germanate anions after hydrogen peroxide addition demonstrates the substitution of initial coordination environment of germanium(IV) atoms and can be caused by peroxide coordination.

The relative stability of the $[Ge_6(\mu\text{-}O)_{12}(OOH)_6]^{6-}$ and $[Ge_6(\mu\text{-}OO)_6(\mu\text{-}O)_6(OH)_6]^{6-}$ anions vs $[Ge_6(\mu\text{-}O)_{12}(OH)_6]^{6-}$ and $[Ge_6(\mu\text{-}O)_{12}(OOH)_6]^{6-}$ anions, respectively, was estimated by DFT calculations. The following gas-phase reactions were considered:

$$[Ge_6(\mu\text{-}O)_{12}(OH)_6]^{6-} + 6H_2O_2 \rightleftarrows [Ge_6(\mu\text{-}O)_{12}(OOH)_6]^{6-} + 6H_2O \quad (1)$$

$$[Ge_6(\mu\text{-}O)_{12}(OOH)_6]^{6-} \rightleftarrows [Ge_6(\mu\text{-}OO)_6(\mu\text{-}O)_6(OH)_6]^{6-} \quad (2)$$

$$[Ge_6(\mu\text{-}OO)_6(\mu\text{-}O)_6(OH)_6]^{6-} + 6H_2O_2 \rightleftarrows [Ge_6(\mu\text{-}OO)_{12}(OH)_6]^{6-} + 6H_2O \quad (3)$$

The relative Gibbs energy $\Delta_rG^0_{298\ K}$ evaluated for reactions 1 − 3 are given Table 1.

Table 1. Theoretical $\Delta_rG^0_{298\ K}$ Values (kJ/mol) of Reactions 1 − 3

reaction	1	2	3
$\Delta_rG^0$298 K	−645.2	−117.1	−177.5

According to Table 1, the hexanuclear peroxogermanate anion is thermodynamically much more stable in the gas phase than its hydroperoxo- and oxogermanate analogues. Results of DFT studies in gas phase may shed light on the transformation of germanate anions in aqueous hydrogen peroxide. Addition of hydrogen peroxide to hydroxogermanate aqueous solution reduces the pH and can induce germanium(IV) polycondensation resulting in hexanuclear μ-oxogermanate $[Ge_6(\mu\text{-}O)_{12}(OH)_6]^{6-}$ (Figure 5A; Scheme S1, structure **I**). Similar germanate structures were previously isolated from aqueous systems.[79] We can suggest that hydrogen peroxide molecules substitute terminal hydroxo ligands in the initial germanate resulting in hydroperoxogermanate anion $[Ge_6(\mu\text{-}O)_{12}(OOH)_6]^{6-}$ (Figure 5B; Scheme S1, structure **II**) similar to the hydroperoxo coordination in hydrogen peroxide solutions of Sn(IV) hydroxocomplexes.[78] $\Delta_rG^0_{298}$ of this reaction in the gas phase is −645.2 kJ/mol.

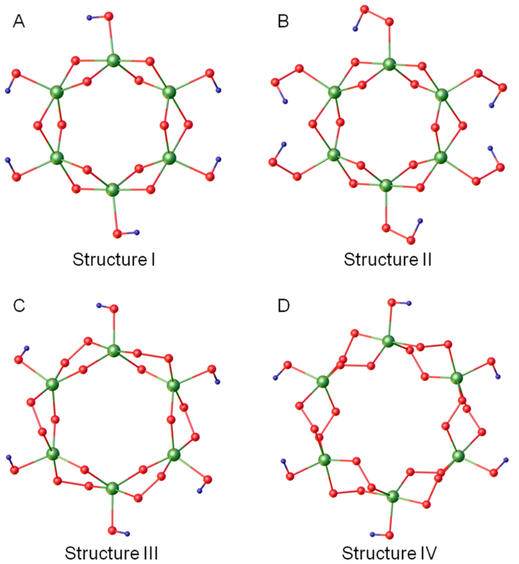

Figure 5. Structures of $[Ge_6(\mu\text{-}O)_{12}(OH)_6]^{6-}$ (A), $[Ge_6(\mu\text{-}O)_{12}(OOH)_6]^{6-}$ (B), $[Ge_6(\mu\text{-}OO)_6(\mu\text{-}O)_6(OH)_6]^{6-}$ (C), and $[Ge_6(\mu\text{-}OO)_{12}(OH)_6]^{6-}$ (D) anions optimized at the B3LYP/6-311G++(d,p) level of theory using LANL2DZ basis set with effective core potential for Ge atoms. Germanium, oxygen, and hydrogen atoms are depicted by green, red, and blue circles, respectively.

Following transformation of hydroperoxogermanate $[Ge_6(\mu\text{-}O)_{12}(OOH)_6]^{6-}$ to μ-peroxogermanate $[Ge_6(\mu\text{-}OO)_6(\mu\text{-}O)_6(OH)_6]^{6-}$ (Figure 5C; Scheme S1, structure **III**) results in additional stabilization (−117 kJ/mol) of the germanium(IV) anion even with taking into account the additional stabilization of the structure **II** by intra-anion hydrogen bonds of hydroperoxo and μ-oxo ligands. The geometry of the optimized structure **III** corresponds well to the geometry of peroxogermanate anion $[Ge_6(\mu\text{-}OO)_6(\mu\text{-}O)_6(OH)_6]^{6-}$ in crystals **1**−**3** (Figure 5C). The Gibbs free energy of the possible following oxo-bridges substitution in structure **III** resulting in peroxogermanate anion $[Ge_6(\mu\text{-}OO)_{12}(OH)_6]^{6-}$ (Figure 5D) is −177.5 kJ/mol, which is relatively small compared to the first stage. Most probably this process requires higher concentration of hydrogen peroxide in the system. Optimized geometry of structures **I**−**IV** and their selected parameters are presented in Figure 5 and Table S4. The thermodynamic stability of the germanium peroxobridged anion is reflected also in the experimentally observed thermal stability. Even after heating of **1**−**3** up to 120 °C, the hexanuclear structure is retained, based on the Raman spectra and permanganometry, though surprisingly we observe water loss rather than peroxide decomposition. A similar phenomenon of water evaporation before peroxide cleavage was demonstrated by Demir (2011) for sodium perborate tetrahydrate.[80]

Studies of crystalline structures often raise questions regarding the relevance of the solid salt to the solution chemistry. The hexanuclear peroxogermanate presented here is a good example for the relevance of the anion structure to the aqueous precursor solution: (i) All three salts (**1**−**3**) share the same hexanuclear anion despite having different crystal packing and different hydrogen bond networks. (ii) The same anionic structure was isolated from a rather wide range of peroxide concentrations (3−20% H_2O_2). (iii) In all cases the isolated compound was the dominant phase in powder XRD studies. A coincidence where the germanium assembles during precipitation to give the same hexanuclear structure from a wide range of solution compositions is unlikely.

Mayer[81] hypothesized a general rule: hydrogen peroxide is a poor ligand to metals, and hydroperoxo and peroxo complexes are formed only after hydrogen peroxide deprotonation in the presence of base. Mayer demonstrated his rule for gallium complexes, but it is easy to see that it holds true also for the ligation activity of borate versus boric acid[82] and hydroxostannate[78] versus tin(IV) salts.

This work shows that Mayer's rule holds true also for germanium ligation, which takes place at high pH only. In order to demonstrate further Mayer's rule for germanium, we have carried out the following simple experiment. We have added 98.3% hydrogen peroxide to germanium tetrachloride. Two stable separated liquid phases were formed (Figure S4). The hydrogen peroxide floated over the liquid $GeCl_4$ phase, and gel formation was not observed. Repeating the test with $GeCl_4$ and 50% H_2O_2 solution resulted in gel formation, but after washing with diethyl ether no peroxide content was found by potassium permanganate titration. In fact, even without rinsing, a dry gel that was obtained by vacuum desiccation at room temperature did not contain any active oxygen. Therefore, we conclude that peroxide coordination to germanium does not occur in acidic conditions in accordance with Mayer's rule.

■ CONCLUDING REMARKS

Three different salts with the hexanuclear peroxogermanate anion $[Ge_6(\mu\text{-}OO)_6(\mu\text{-}O)_6(OH)_6]^{6-}$ were isolated from different aqueous solutions of widely different compositions, demonstrating the stability of the hexanuclear peroxogermanate anion in basic hydrogen peroxide−water solutions.

The hexanuclear peroxogermanate anion $[Ge_6(\mu\text{-}OO)_6(\mu\text{-}O)_6(OH)_6]^{6-}$ is the first structurally characterized strictly inorganic germanium peroxo complex, the first p-block element multinuclear peroxocomplex isolated from aqueous solution, and the first end-on $\mu-\eta^1:\eta^1\text{-}O_2^{2-}$ multinuclear complex isolated from aqueous solution. It demonstrates for the first time aqueous hydrogen peroxide induced nontransition element polycondensation by the peroxobridging mechanism. Thus, we can conclude that peroxobridging skeleton can play a more than expected role in the p-block element polycondensations and sol and film formations.

The hexanuclear peroxogermanate was isolated only from basic aqueous solution, serving as another example for Mayer's rule regarding the poor metal ligation ability of hydrogen peroxide under acidic conditions.

■ ASSOCIATED CONTENT

Ⓢ Supporting Information

The Supporting Information is available free of charge on the ACS Publications website at DOI: 10.1021/acs.inorgchem.5b01293.

> X-ray powder diffractograms of **1**−**3**, Raman spectra, NMR spectra, and additional computational data. An illustration of two-phase formation by mixing $GeCl_4$ and 98.3% H_2O_2 vs rapid gelation taking place after the addition of 50% H_2O_2 to germanuim chloride (PDF)
>
> Crystallographic information (CIF)
>
> Crystallographic information (CIF)

■ AUTHOR INFORMATION

Corresponding Authors

*E-mail: ovadia@mail.huji.ac.il.
*E-mail: prikhman@gmail.com.

Notes

The authors declare no competing financial interest.

■ ACKNOWLEDGMENTS

This Research is conducted by NTU-HUJ-BGU Nanomaterials for Energy and Water Management Programme under the Campus for Research Excellence and Technological Enterprise (CREATE), that is supported by the National Research Foundation, Prime Minister's Office, Singapore. The financial support of Israel Research Foundation and the Ministry of Science, Technology and Space is thankfully acknowledged. We thank the Harvey M. Krueger Family Center for Nanoscience and Nanotechnology of the Hebrew University of Jerusalem and the Israel Science Foundation. We thank the Russian Foundation for Basic Research (grant 14-03-00279). A.G.M. thankfully acknowledges a Golda Meir Postdoctoral Fellowship, A.A.M. thankfully acknowledges a Valazzi−Pikovsky Fellowship and the Council on Grants of the President of the Russian Federation (MK-5847.2014.3, SP-995.2015.1) for support.

REFERENCES

(1) Piquemal, J.-Y.; Briot, E.; Bregeault, J.-M. *Dalton Trans.* **2013**, *42*, 29−45.

(2) Wolanov, Y.; Shurki, A.; Prikhodchenko, P. V.; Tripol'skaya, T. A.; Novotortsev, V. M.; Pedahzur, R.; Lev, O. *Dalton Trans.* **2014**, *43*, 16614−16625.

(3) Sladkevich, S.; Gutkin, V.; Lev, O.; Legurova, E.; Khabibulin, D.; Fedotov, M.; Uvarov, V.; Tripol'skaya, T.; Prikhodchenko, P. *J. Sol-Gel Sci. Technol.* **2009**, *50*, 229−240.

(4) Sladkevich, S.; Mikhaylov, A. A.; Prikhodchenko, P. V.; Tripol'skaya, T. A.; Lev, O. *Inorg. Chem.* **2010**, *49*, 9110−9112.

(5) Sladkevich, S.; Gun, J.; Prikhodchenko, P. V.; Gutkin, V.; Mikhaylov, A. A.; Novotortsev, V. M.; Zhu, J. X.; Yang, D.; Hng, H. H.; Tay, Y. Y.; Tsakadze, Z.; Lev, O. *Nanotechnology* **2012**, *23*, 485601.

(6) Prikhodchenko, P. V.; Gun, J.; Sladkevich, S.; Mikhaylov, A. A.; Lev, O.; Tay, Y. Y.; Batabyal, S. K.; Yu, D. Y. W. *Chem. Mater.* **2012**, *24*, 4750−4757.

(7) Yu, D. Y. W.; Prikhodchenko, P. V.; Mason, C. W.; Batabyal, S. K.; Gun, J.; Sladkevich, S.; Medvedev, A. G.; Lev, O. *Nat. Commun.* **2013**, *4*, 2922.

(8) Prikhodchenko, P. V.; Yu, D. Y. W.; Batabyal, S. K.; Uvarov, V.; Gun, J.; Sladkevich, S.; Mikhaylov, A. A.; Medvedev, A. G.; Lev, O. *J. Mater. Chem. A* **2014**, *2*, 8431−8437.

(9) Vener, M. V.; Medvedev, A. G.; Churakov, A. V.; Prikhodchenko, P. V.; Tripol'skaya, T. A.; Lev, O. *J. Phys. Chem. A* **2011**, *115*, 13657−13663.

(10) Prikhodchenko, P. V.; Medvedev, A. G.; Tripol'skaya, T. A.; Churakov, A. V.; Wolanov, Y.; Howard, J. A. K.; Lev, O. *CrystEngComm* **2011**, *13*, 2399−2407.

(11) Churakov, A. V.; Prikhodchenko, P. V.; Howard, J. A. K.; Lev, O. *Chem. Commun.* **2009**, 4224−4226.

(12) Churakov, A. V.; Prikhodchenko, P. V.; Howard, J. A. K. *CrystEngComm* **2005**, *7*, 664−669.

(13) Kinrade, S. D.; Holah, D. G.; Hill, G. S.; Menuz, K. E.; Smith, C. R. *J. Wood Chem. Technol.* **1995**, *15*, 203−222.

(14) Zeglinski, J.; Cabaj, A.; Strankowski, M.; Czerniak, J.; Haponiuk, J. T. *Colloids Surf., B* **2007**, *54*, 165−172.

(15) Zeglinski, J.; Piotrowski, G. P.; Piekos, R. *J. Mol. Struct.* **2006**, *794*, 83−91.

(16) Sladkevich, S.; Gun, J.; Prikhodchenko, P. V.; Gutkin, V.; Mikhaylov, A. A.; Medvedev, A. G.; Tripol'skaya, T. A.; Lev, O. *Carbon* **2012**, *50*, 5463−5471.

(17) Coggins, M. K.; Sun, X.; Kwak, Y.; Solomon, E. I.; Rybak-Akimova, E.; Kovacs, J. A. *J. Am. Chem. Soc.* **2013**, *135*, 5631−5640.

(18) Bhula, R.; Gainsford, G. J.; Weatherburn, D. C. *J. Am. Chem. Soc.* **1988**, *110*, 7550−7552.

(19) Bossek, U.; Weyhermueller, T.; Wieghardt, K.; Nuber, B.; Weiss, J. *J. Am. Chem. Soc.* **1990**, *112*, 6387−6388.

(20) Tolis, E. I.; Helliwell, M.; Langley, S.; Raftery, J.; Winpenny, R. E. P. *Angew. Chem., Int. Ed.* **2003**, *42*, 3804−3808.

(21) Zhang, X.; Furutachi, H.; Fujinami, S.; Nagatomo, S.; Maeda, Y.; Watanabe, Y.; Kitagawa, T.; Suzuki, M. *J. Am. Chem. Soc.* **2005**, *127*, 826−827.

(22) Kim, K.; Lippard, S. J. *J. Am. Chem. Soc.* **1996**, *118*, 4914−4915.

(23) Dong, Y.; Yan, S.; Young, V. G.; Que, L. *Angew. Chem., Int. Ed. Engl.* **1996**, *35*, 618−620.

(24) Ookubo, T.; Sugimoto, H.; Nagayama, T.; Masuda, H.; Sato, T.; Tanaka, K.; Maeda, Y.; Okawa, H.; Hayashi, Y.; Uehara, A.; Suzuki, M. *J. Am. Chem. Soc.* **1996**, *118*, 701−702.

(25) Wang, B. C.; Schaefer, W. P. *Science* **1969**, *166*, 1404−1406.

(26) Southon, P. D.; Price, D. J.; Nielsen, P. K.; McKenzie, C. J.; Kepert, C. J. *J. Am. Chem. Soc.* **2011**, *133*, 10885−10891.

(27) Bouwman, E.; Driessen, W. L. *J. Am. Chem. Soc.* **1988**, *110*, 4440−4441.

(28) Seo, J. S.; Hynes, R. C.; Williams, D.; Chin, J.; Sung, N.-D. *J. Am. Chem. Soc.* **1998**, *120*, 9943−9944.

(29) Gavrilova, A. L.; Qin, C. J.; Sommer, R. D.; Rheingold, A. L.; Bosnich, B. *J. Am. Chem. Soc.* **2002**, *124*, 1714−1722.

(30) Givaja, G.; Volpe, M.; Edwards, M. A.; Blake, A. J.; Wilson, C.; Schröder, M.; Love, J. B. *Angew. Chem., Int. Ed.* **2007**, *46*, 584−586.

(31) Fukuzumi, S.; Mandal, S.; Mase, K.; Ohkubo, K.; Park, H.; Benet-Buchholz, J.; Nam, W.; Llobet, A. *J. Am. Chem. Soc.* **2012**, *134*, 9906−9909.

(32) Reinaud, O. M.; Yap, G. P. A.; Rheingold, A. L.; Theopold, K. H. *Angew. Chem., Int. Ed. Engl.* **1995**, *34*, 2051−2052.

(33) Shiren, K.; Ogo, S.; Fujinami, S.; Hayashi, H.; Suzuki, M.; Uehara, A.; Watanabe, Y.; Moro-oka, Y. *J. Am. Chem. Soc.* **2000**, *122*, 254−262.

(34) Jacobson, R. R.; Tyeklar, Z.; Farooq, A.; Karlin, K. D.; Liu, S.; Zubieta, J. *J. Am. Chem. Soc.* **1988**, *110*, 3690−3692.

(35) Würtele, C.; Sander, O.; Lutz, V.; Waitz, T.; Tuczek, F.; Schindler, S. *J. Am. Chem. Soc.* **2009**, *131*, 7544−7545.

(36) Hoppe, T.; Schaub, S.; Becker, J.; Würtele, C.; Schindler, S. *Angew. Chem., Int. Ed.* **2013**, *52*, 870−873.

(37) Baranovskii, I. B.; Zhilyaev, A. N.; Dikareva, L. M.; Rotov, A. V. *Russ. J. Inorg. Chem.* **1986**, *31*, 2892−2901.

(38) Huacuja, R.; Graham, D. J.; Fafard, C. M.; Chen, C.-H.; Foxman, B. M.; Herbert, D. E.; Alliger, G.; Thomas, C. M.; Ozerov, O. V. *J. Am. Chem. Soc.* **2011**, *133*, 3820−3823.

(39) Akita, M.; Miyaji, T.; Moro-oka, Y. *Chem. Commun.* **1998**, 1005−1006.

(40) Xiao, J.; Santarsiero, B. D.; Vaartstra, B. A.; Cowie, M. *J. Am. Chem. Soc.* **1993**, *115*, 3212−3220.

(41) Davies, M. S.; Hambley, T. W. *Inorg. Chem.* **1998**, *37*, 5408−5409.

(42) Kamata, K.; Kuzuya, S.; Uehara, K.; Yamaguchi, S.; Mizuno, N. *Inorg. Chem.* **2007**, *46*, 3768−3774.

(43) Roşca, D.-A.; Wright, J. A.; Hughes, D. L.; Bochmann, M. *Nat. Commun.* **2013**, *4*, 2167.

(44) Bassil, B. S.; Mal, S. S.; Dickman, M. H.; Kortz, U.; Oelrich, H.; Walder, L. *J. Am. Chem. Soc.* **2008**, *130*, 6696−6697.

(45) Chernyshov, B. N.; Didenko, N. A.; Bukvetskii, B. V.; Gerasimenko, A. V.; Kavun, V. Y.; Sergienko, S. S. *Russ. J. Inorg. Chem.* **1989**, *34*, 2786−2794.

(46) Davies, A. G. *Tetrahedron* **2007**, *63*, 10385−10405.

(47) Uhl, W.; Halvagar, M. R.; Layh, M. *Chem. Commun.* **2009**, 4269−4271.

(48) Uhl, W.; Halvagar, M. R. *Angew. Chem., Int. Ed.* **2008**, *47*, 1955−1957.

(49) Uhl, W.; Melle, S.; Prott, M. *Z. Anorg. Allg. Chem.* **2005**, *631*, 1377−1382.

(50) Cardin, C. J.; Cardin, D. J.; Devereux, M. M.; Convery, M. A. *J. Chem. Soc., Chem. Commun.* **1990**, 1461−1462.

(51) Chorley, R. W.; Hitchcock, P. B.; Lappert, M. F. *J. Chem. Soc., Chem. Commun.* **1992**, 525−526.

(52) Schneider, J. J.; Hagen, J.; Heinemann, O.; Bruckmann, J.; Kruger, C. *Thin Solid Films* **1997**, *304*, 144−148.

(53) Breunig, H. J.; Kruger, T.; Lork, E. *Angew. Chem., Int. Ed. Engl.* **1997**, *36*, 615−617.

(54) Breunig, H.; Kruger, T.; Lork, E. *J. Organomet. Chem.* **2002**, *648*, 209−213.

(55) Sharutin, V. V.; Pakusina, A. P.; Smirnova, S. A.; Sharutina, O. K.; Platonova, T. P.; Pushilin, M. A.; Gerasimenko, A. V. *Russ. J. Coord. Chem.* **2004**, *30*, 314−321.

(56) Back, T. G.; Kuzma, D. A.; Parvez, M. *J. Org. Chem.* **2005**, *70*, 9230−9236.

(57) Balazs, L.; Breunig, H. J.; Lork, E.; Soran, A.; Silvestru, C. *Inorg. Chem.* **2006**, *45*, 2341−2346.

(58) Carrondo, M. A. A. F. de C. T.; Skapski, A. C. *Acta Crystallogr., Sect. B: Struct. Crystallogr. Cryst. Chem.* **1978**, *34*, 3551−3554.

(59) Kako, M.; Akasaka, T.; Ando, W. *J. Chem. Soc., Chem. Commun.* **1992**, 457−458.

(60) Ando, W.; Kako, M.; Akasaka, T. *J. Chem. Soc., Chem. Commun.* **1992**, 458−460.

(61) Cui, C. M.; Olmstead, M. M.; Fettinger, J. C.; Spikes, G. H.; Power, P. P. *J. Am. Chem. Soc.* **2005**, *127*, 17530−17541.

DOI: 10.1021/acs.inorgchem.5b01293

(62) Masamune, S.; Batcheller, S. A.; Park, J.; Davis, W. M.; Yamashita, O.; Ohta, Y.; Kabe, Y. *J. Am. Chem. Soc.* **1989**, *111*, 1888−1889.

(63) Wang, X.; Peng, Y.; Olmstead, M. M.; Fettinger, J. C.; Power, P. P. *J. Am. Chem. Soc.* **2009**, *131*, 14164−14165.

(64) Allen, F. *Acta Crystallogr., Sect. B: Struct. Sci.* **2002**, *58*, 380−388.

(65) Belsky, A.; Hellenbrandt, M.; Karen, V. L.; Luksch, P. *Acta Crystallogr., Sect. B: Struct. Sci.* **2002**, *58*, 364−369.

(66) Shklover, V. E.; Ad'yaasuren, P.; Tsinker, I.; Yablokov, V. A.; Ganyushkin, A. V.; Struchkov, Y. T. *J. Struct. Chem.* **1980**, *21*, 342−347.

(67) Wolanov, Y.; Lev, O.; Churakov, A. V.; Medvedev, A. G.; Novotortsev, V. M.; Prikhodchenko, P. V. *Tetrahedron* **2010**, *66*, 5130−5133.

(68) Frisch, M. J.; Trucks, G. W.; Schlegel, H. B.; Scuseria, G. E.; Robb, M. A.; Cheeseman, J. R.; Scalmani, G.; Barone, V.; Mennucci, B.; Petersson, G. A.; Nakatsuji, H.; Caricato, M.; Li, X.; Hratchian, H. P.; Izmaylov, A. F.; Bloino, J.; Zheng, G.; Sonnenberg, J. L.; Hada, M.; Ehara, M.; Toyota, K.; Fukuda, R.; Hasegawa, J.; Ishida, M.; Nakajima, T.; Honda, Y.; Kitao, O.; Nakai, H.; Vreven, T.; Montgomery Jr., J. A.; Peralta, J. E.; Ogliaro, F.; Bearpark, M. J.; Heyd, J.; Brothers, E. N.; Kudin, K. N.; Staroverov, V. N.; Kobayashi, R.; Normand, J.; Raghavachari, K.; Rendell, A. P.; Burant, J. C.; Iyengar, S. S.; Tomasi, J.; Cossi, M.; Rega, N.; Millam, N. J.; Klene, M.; Knox, J. E.; Cross, J. B.; Bakken, V.; Adamo, C.; Jaramillo, J.; Gomperts, R.; Stratmann, R. E.; Yazyev, O.; Austin, A. J.; Cammi, R.; Pomelli, C.; Ochterski, J. W.; Martin, R. L.; Morokuma, K.; Zakrzewski, V. G.; Voth, G. A.; Salvador, P.; Dannenberg, J. J.; Dapprich, S.; Daniels, A. D.; Farkas, Ö.; Foresman, J. B.; Ortiz, J. V.; Cioslowski, J.; Fox, D. J. *Gaussian 09*, Gaussian, Inc.: Wallingford, CT, 2009.

(69) Savariault, J. M.; Lehmann, M. S. *J. Am. Chem. Soc.* **1980**, *102*, 1298−1303.

(70) Fritchie, C. J., Jr.; McMullan, R. K. *Acta Crystallogr., Sect. B: Struct. Crystallogr. Cryst. Chem.* **1981**, *37*, 1086−1091.

(71) Chauchene, S.; Jaouadi, K.; Mhiri, T.; Zouari, N. *Adv. Chem.* **2014**, *10*, 2944−2954.

(72) Karadjova, V.; Wildner, M.; Stoilova, D. *Int. Res. J. Pure Appl. Chem.* **2015**, *5*, 245−262.

(73) Orera, A.; Sanjuan, M. L.; Kendrick, E.; Orera, V. M.; Slater, P. R. *J. Mater. Chem.* **2010**, *20*, 2170−2175.

(74) Henderson, G. S.; Fleet, M. E. *J. Non-Cryst. Solids* **1991**, *134*, 259−269.

(75) Sigaev, V. N.; Gregora, I.; Pernice, P.; Champagnon, B.; Smelyanskaya, E. N.; Aronne, A.; Sarkisov, P. D. *J. Non-Cryst. Solids* **2001**, *279*, 136−144.

(76) Arnau, J. L.; Giguere, P. A.; Abe, M.; Taylor, R. C. *Spectrochim. Acta* **1974**, *30A*, 777−796.

(77) Chumaevskii, N. A.; Prikhodchenko, P. V.; Minaeva, N. A.; Ippolitov, E. G. *Russ. J. Inorg. Chem.* **2003**, *48*, 1538−1540.

(78) Churakov, A. V.; Sladkevich, S.; Lev, O.; Tripol'skaya, T. A.; Prikhodchenko, P. V. *Inorg. Chem.* **2010**, *49*, 4762−4764.

(79) Mafra, L.; Paz, F. A. A.; Shi, F.-N.; Ferreira, R. A. S.; Carlos, L. D.; Trindade, T.; Fernandez, C.; Klinowski, J.; Rocha, J. *Eur. J. Inorg. Chem.* **2006**, 4741−4751.

(80) Demir, H. *Korean J. Chem. Eng.* **2011**, *28*, 2002−2008.

(81) DiPasquale, A. G.; Mayer, J. M. *J. Am. Chem. Soc.* **2008**, *130*, 1812−1813.

(82) Flanagan, J.; Griffith, W. P.; Powell, R. D.; West, A. P. *J. Chem. Soc., Dalton Trans.* **1989**, 1651−1655.